Silicon (2023) 15:7415–7429
https://doi.org/10.1007/s12633-023-02593-2

RESEARCH

# Polyphenol-compounds From Green Synthesis of Antimicrobial property of Silver Nanoparticles using *Eichhornia crassipes*: Characterization and Applications

**Azhagu Madhavan Sivalingam[1] · Arjun Pandian[2] · Sumathy Rengarajan[3] · Raju Ramasubbu[4]**

Received: 26 May 2023 / Accepted: 5 July 2023 / Published online: 15 July 2023
© Springer Nature B.V. 2023

## Abstract

In this study, the authors aimed to expand a sustainable and gainful methodology for the purpose of synthesizing silver nanoparticles (AgNPs) using polyphenol bioactive compounds extracted from *Eichhornia crassipes.* The eco-friendliness of this method was also emphasized. The ethanol leaf extract with silver nitrate solution heated and filtered then the AgNPs produced were extensively the samples were thoroughly nanoparticles charaterized using a range of analytical techniques, including UV (nanoparticles wavelength measured), FTIR (functional groups), SEM (morphology, size, range, etc.,), TEM (morphological size of nanoparticles), XRD (crystaline sturcture), EDX (elemental composition), and AFM (irregular shape). In results the characterization process revealed the presence of secondary metabolites, total phenol content (TPC) observed that the highest value of 212.47 ± 7.07 (GAE). Additionally, through GC–MS analysis 12 major bioactive compounds were identified; In UV-Visible spectrum analysized its confirmed that size of nanoparticles in 448 nm absorption of the surface Plasmon resonance band by observed. The dimension of AgNPs was analyzed through SEM was found 11 nm. TEM and SAED analyses revealed the high crystallinity of AgNPs with homogeneous polycrystalline components and lattice spacing at 0.295. XRD patterns displayed four Bragg reflections at 38.45 (111), 46.35 (200), 64.75 (220), and 78.05 (301). Energy synthesis in EDX was observed in 8.79 nm. The AFM analysis the irregular shapes noticed. The synthesized AgNPs tested antimicrobial properties against various strains of microorganisms, including *Staphylococcus aureus* and *Fusarium graminium*. The synthesized AgNPs demonstrated potent antimicrobial activity, as evidenced by the highest zones of inhibition observed against *Staphylococcus aureus* (16.8 ± 0.03 mm) bacteria and *Fusarium graminium* (12.01 ± 0.01 mm) fungi at a concentration of 80 µg/mL. Our findings concluded that polyphenolic compounds are mostly in high amount reported in fresh fruits and vegetables so for that its having biological properties, same polyphenolic compounds we identified from leaf ethanolic extract of *E. crassipes*.

**Keywords** Antimicrobial · Anticancer · Elemental composition · Green synthesis · Phenolic content

✉ Azhagu Madhavan Sivalingam
mathavan062@gmail.com

[1] Natural Products & Nanobiotechnology Research Lab, Department of Community Medicine, Saveetha Medical College, Saveetha Institute of Medical and Technical Sciences (SIMATS), Thandalam, Chennai 602105, Tamil Nadu, India

[2] Department of Research and Innovation, Institute of Biotechnology, Saveetha School of Engineering (SSE), Saveetha Institute of Medical and Technical Sciences (SIMATS), Thandalam, Chennai 602105, Tamil Nadu, India

[3] Department of Biotechnology, Valliammal College for Women, E -9; Anna Nagar East, Chennai 602105, Tamil Nadu, India

[4] Department of Biology, The Gandhigram Rural Institute (Deemed to Be University), Gandhigram, Dindugal 624 302, Tamil Nadu, India

## 1 Introduction

Water hyacinth (*Eichhornia crassipes*) is an aquatic plant species that is well-known for its rapid spread in water environments, its used for removal of contaminants from water bodies its cost-effective and environmentally pleasant method. It has excellent properties for growing in contaminated water and absorbing inorganic toxicants. Biomass can be used by cultivating plants in contaminated environments or employing dry biomass as an adsorbent for natural compounds in nanomaterial synthesis. [1, 2]. *E. crassipes* plants can trap organic matter, and the bacterial colonies on their surface can lead to the formation of methylmercury ($CH_3Hg$). The plant materials also exhibit plasmon resonance peaks around the morphological diameter, as seen through UV–Visible absorption. Additionally, there is connectivity of (AgNPs) silver nanoparticles synthesized surface of the *E. crassipes* plant materials [3, 4]. In comparison to chemical synthesis, green synthesis methods have biocompatibility and can reduce ions into nano-sized atoms without the use of harmful chemicals [5]. The application of microbes and plants for the synthesized of nanoparticles offers a promising avenue in biological methods [6]. AgNPs (silver nanoparticles) have bactericidal characteristics and may emit Ag+, which is harmful to bacteria [7]. Various biologically methods for the *Trigonella incise* synthesizing are currently focusing on the green synthesis of silver nanoparticles (Ag NPs) and studying their potential antimicrobial properties [8]. The combined effect of chitosan and polyphenols derived from seaweed in synthesizing (AgNPs) silver nanoparticles with enhanced antibacterial activity. The biosynthesis of AgNPs was carried out the possess of properties a green synthetic route, utilizing the synergistic potential of chitosan and seaweed-derived polyphenols [9]. The production of polyphenol-coated silver nanoparticles (PAgNPs) through the utilization of an aqueous extract obtained from *yerba mate tea* energy of (Ilex paraguariensis) as a natural stabilizing agent and reducing [10]. This study focus on the phenol red removal of green synthesis of Ag NPs using *Eichhornia crassipes* ethanol extracts, synthesized AgNPs exhibit distinct morphological, optical, and geometrical characteristics by analytical techniques. These techniques such as UV–Visible Spectrophotometer, FTIR, TEM, SEM, XRD, EDX, and AFM. Furthermore, the antimicrobial properties of the synthesized silver nanoparticles AgNPs was assessed.

## 2 Material methods

### 2.1 Sample collection and preparation of *Eichhornia crassipes* extract for phytochemical analysis

The medicinal plant *Eichhornia crassipes* was collected from the post in the Saliyamangalam, Thanjavur District, Tamil Nadu, India, collected plant materials shade dried. After collecting the plant materials using, they were dried in the shade and utilized for phytochemical analysis. To extract the phytochemicals, a Soxhlet extractor was utilized with 500 g of dried *E. crassipes* leaf extract. The extraction process involved exposing the sample to 1250 ml of ethanol solvent for a duration of two hours. Following this, the obtained crude *E. crassipes* extract was filtered and individually using Whatman No. 41 filter paper. The resulting filtrate was then evaporated at 60 °C using a rotating evaporator to obtain a concentrated sample. This concentrated sample was subsequently stored for future analysis, ensuring its preservation. Collected crude *Eichhornia crassipes* leaf ethanol extract stored for further analysis.

### 2.2 Estimation of Total Phenol Content

**Expending** The strength of character of the total phenolic content was carried out Expending a slightly modified Folin-Ciocalteu technique. Initially, *E. crassipes* leaf weighing 200 mg were homogenized with a 1:1 (v/v) mixture of acetone and water (2 mL) at 25 °C for 1 h. The obtained mixture was subjected to centrifugation at 6000 rpm for 10 min, followed by vacuum drying. Then, a combination of 9 µL of the *E. crassipes* extract (1 mg/mL) and 109 µL of Folin-Ciocalteu reagent was prepared. After incubating for 3 min at 25 °C, a solution of 180 µL of 7.5% (w/v) Na2CO3 was added. The mixture was left to stand for 5 min at 50 °C and subsequently cooled to 25 °C. Finally, the absorbance was measured at 760 nm using the Zenyth 200rt Microplate Reader. To calculate the total phenolic content, a gallic acid standard curve was employed, and the results were communicated as milligrams of Gallic Acid Equivalents (GAE) per gram of fresh weight (FW). It is important of the ensure accuracy and reliability of the measurements, the analysis was conducted on triplicate samples. [11].

### 2.3 Gas chromatography with Mass spectrometry

The *E. crassipes* samples were diluted in n-hexane (10 µL/300 µL) for analysis used to gas chromatography (GC) and gas chromatography-mass spectrometry (GC–MS). GC analysis was performed on an Agilent Technologies 7890 Apparatus, equipped with a split-splitless injector and an HP-5 column (30 m × 0.32 mm, film thickness 0.25 µm), coupled with a flame ionization detector. Helium was used as the carrier gas with a flow rate of 1 mL/min. The injector and detector temperatures were set at 250 ºC and 280 ºC, respectively. The column temperature was programmed to increase from 40 ºC to 260 ºC at a rate of 4 ºC/min. The percentage composition of the *E. crassipes* samples was determined by analyzing peak areas without applying correction factors. For GC–MS analysized, an HPG 1800 C Series II GCD analytical system with an HP-5MS column was utilized in the mass spectra were recorded in Electron Ionization (EI) mode with an energy of 70 eV, covering the mass-to-charge ratio (m/z) range of 40–450. The identification of volatile constituents in the oils involved calculating in their Kovats retention index (RI) and comparing of their mass spectra with reference compounds from the used to Nirst and Willey libraries [11].

### 2.4 Synthesises silver nanoparticles from *Eichhornia crassipes*

The preparation of the ethanol extract from *E. crassipes* achieve this, 15 g of rinsed and dried plant samples were refluxed in 150 mL of deionized water at 60 °C with continuous shaking for 15 min. This refluxing process resulted in the formation of a clear, pale yellow solution. Subsequently, the solution was allowed to cool to room temperature and then filtered using Whatman No.1 filter paper (Whatman, Fisher Scientific, Pittsburgh, PA, USA) to eliminate any suspended particles. The resulting *E. crassipes* extract was divided into two portions: one portion was stored at 4–8 °C for future use, while the other portion underwent vacuum drying in an oven at 40 °C for 48 h. This drying procedure yielded a powdered lemon zest extract suitable for the FTIR analysis [12].

### 2.5 Green Synthesis of Silver Nanoparticles

The green synthesis of (AgNPs) silver nanoparticles with slight modifications. In a 250 mL flask, 10 mL of *E. crassipes* ethanolic extraction was mixed with 90 mL of freshly prepared silver nitrate aqueous solution (AgNO3) at a concentration of 1 mM. The mixture was stimulated using a hot plate magnetic stirrer at 200 rpm and 60 °C in the absence of light. After 30 min, the solution exhibited turbidity and acquired a reddish-brown color, indicating the successful formation of silver nanoparticles. To purify the AgNPs, the mixture underwent centrifugation three times at 15,000 rpm for 20 min, resulting in the formation of a dark brown precipitate. The using precipitate was subsequently washed with sterilized water and methanol, and then dried to obtain pure silver nanoparticles. The optimization of synthesis conditions involved varying to the concentration of the *E. crassipes* plant extract, the contact time, and the AgNO3 concentration. The size and morphology of the synthesized AgNPs were analyzed using UV–visible spectroscopy [13].

## 3 Characterization of silver nanoparticles [AgNPs]

### 3.1 Spectroscopy Characterization of Green AgNPs

#### 3.1.1 UV–Vis spectrophotometry and FT-IR

The surface plasmon resonance (SPR) of the silver nanoparticles (AgNPs) synthesized through green methods was examined used to a UV–Vis spectrophotometer (Thermo Fisher Scientific UviLine 9400C, Loughborough, UK). To analyze the functional groups and surface chemistry of the dried *E. crassipes* extract obtained from Citrus limon zest and the synthesized AgNPs, FT-IR spectroscopy analysis was conducted using an Agilent Cary 640 FTIR spectrometer. The spectra were recorded to at room temperature in the range of 400–4000 cm-1. Furthermore, the particle size and dynamic light scattering of the AgNPs were determined using a nano zeta sizer instrument (Malvern) to at a temperature of 25 °C and a detection angle of 90 degrees [13].

#### 3.1.2 X-ray Differaction method (XRD)

XRD measurements were conducted using a Philips (PW 1710) Diffractometer operating at 40 kV and 40 mA, with Cu(Kα) radiation (λ = 1.5406 Å), covering a diffraction angle (2θ) range of 10° to 90°. The purpose of this analysis was to determine in the crystalline nature and purity of the (AgNPs) silver nanoparticles. The particle size of the AgNPs was calculated using the Scherrer equation ($D = K\lambda/\beta\cos\theta$), where D represents the average crystallite size. The Scherrer constant (K), typically ranging from 0.68 to 2.08, was set to 0.94 for cubic symmetry spherical crystallites. The X-ray wavelength (λ) was denoted as CuKα = 1.5406 Å, β represented the line broadening at the full width at half maximum (FWHM) in radians, and θ indicated the Bragg angle in degrees. Additionally, Bragg's equation ($n\lambda = 2d\sin\theta$) was employed to calculate the d-spacing value, which is related to the diffraction of light from particles [14].

### 3.1.3 Scanning Electron Microscopy (SEM), X-ray spectrometer (EDX) and Atomic Force Microscope (AFM)

The morphology and elemental composition of the silver nanoparticles (AgNPs) were investigated using a JEOL JSM-5910 scanning electron microscope (SEM) in conjunction with an energy dispersive X-ray spectrometer (EDX). The SEM analysis was performed at an acceleration voltage of 20 kV, with a resolution of × 30,000 for image capture. In addition, the morphological form, size, and shape of the silver nanoparticles were investigated using a transmission electron microscope (TEM) (Zeiss EM 900 instrument model). Furthermore, the Atomic Force Microscopy (AFM) measurement was conducted morphology of the *E. crassipes* samples was characterized using an AFM-Agilent 7500 AFM/SPM 3D operating in tapping mode. The maximum scan areas available were 90 µm × 90 µm. The *E. crassipes* sample and cantilever positioning were accomplished using a charge-coupled device monitor. Scans were conducted at different widths, including 10 µm, 5 µm, 2 µm, and 1.2 µm. The obtained phase and height images were analyzed using software based on Asylum Research IGOR PRO.[15, 16].

## 3.2 Antimicrobial activity

The preparation of antimicrobial activity of the ethanolic *E. crassipes* leaf extract was assessed in vitro using the disk diffusion method. Sterile petri dishes with a diameter of 90 mm were filled with Muller Hinton Agar (MHA) medium and allowed to solidify at room temperature. Cultures of four human pathogenic bacterial strains, namely *Pseudomonas aeruginosa, Salmonella typhi*, *Staphylococcus aureus* and *Klebsiella pneumonia*, were evenly spread on the surface of the MHA plates using swabs. To create wells in the Mueller–Hinton agar (MHA), a sterile cork borer with an 8 mm diameter was used. Various concentrations (20, 40, 60, 80 µg/mL) of the ethanolic leaf extract of *E. crassipes* were into loaded the wells used as a sterile micropipette. The inoculated plates were initially incubated at room temperature for 15 min, followed by further incubation at 37 °C for 24 h. To ensure consistency, the turbidity of the bacterial cultures was adjusted with sterile broth to match the 0.5 McFarland standards. After the incubation period, at the diameter of the growth-free zones was measured into assess the antibacterial activity, including the well diameter, was recorded as inhibition zones to measure the antimicrobial activity [17, 18].

**Antifungal activity** The antifungal activity of the ethanolic *E. crassipes* leaf extract was evaluated following the described protocol. Sterile petri dishes with a diameter of 90 mm were prepared and filled with Sabouraud Dextrose Agar (SDA). The objective was to assess the antifungal efficacy of the E. crassipes extract against three human pathogenic fungi: *Candida albicans*, *Fusarium graminearum*, and *Alternaria alternata*. Fresh fungal cultures were evenly spread on the surface of in the SDA plates using a sterile swab. Wells, measuring 8 mm in diameter, were carefully created in the SDA using a sterile cork borer. Subsequently, different concentrations of the *E. crassipes* leaf extract (20, 40, 60, 80 µg/mL) were into loaded the wells using a sterile micropipette. The plates were then incubated at room temperature for 15 min, followed by further incubation at 37 °C for 24 h. After the incubation period, the plates were examined to identify any zones of growth inhibition. The diameter of the growth-free zones, including the well diameter, measured was recorded and inhibition zone. The percentage of inhibition to calculate in the following mthods of formula was applied: % of inhibition = (zone of inhibition diameter in mm / petri plate diameter in mm) × 100 [17].

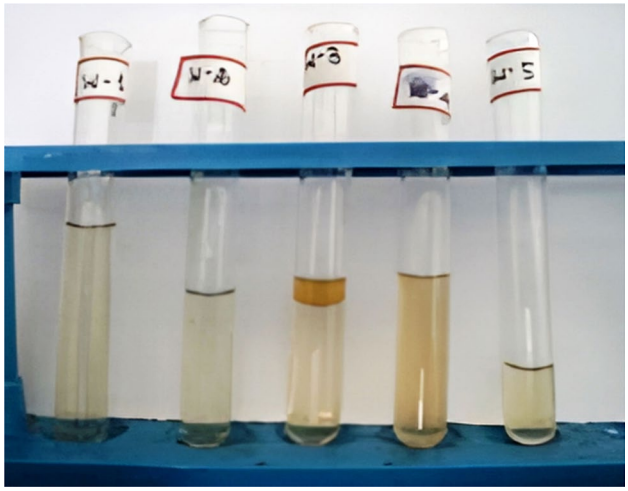

**Fig. 1** Phytochemical analysis of secondary metabolites

**Statistical analysis** The statistical analysis employed tools in this study consisted of conducting a One-way Analysis of Variance (ANOVA) to the assess significance of differences among the various treatment groups. To determine

**Table 1** Phytochemical analysis of plant leaf ethanolic extract

| S.NO | Secondary metabolites | Ethanol |
|---|---|---|
| 1 | Tannin | + |
| 2 | Alkaloids | + |
| 3 | Flavonoids | + |
| 4 | Steroids | + |
| 5 | Poly-phenol | + |

**Table 2** TPC of plant Extract *E.crassipes* using ethanol solution

| S.No | Solvents | TPC (mg $GAE^{-1}$) |
|---|---|---|
| 1 | Ethanol | 212.47 ± 7.07 |

specific variations between the different treatment groups, Duncan's Multiple Range Test (DMRT) was conducted using SPSS (Statistical Package for the Social Sciences) software, Version 16.0, with a significance level of 5%. Results were deemed statistically significant if the p-value was below 0.05 ($P < 0.05$) [19].

## 4 Result and Discussion

### 4.1 Phytochemical testing

In qualitative phytochemical analysis of secondary metabolites tested in ethanolic *E. crassipes* leaf extract of *E. crassipes,* plant extract unveiled the presence of bioactive compounds; flavonoids, alkaloids, tannins, and saponins polyphenols, identified secondary metabolites are recognized for its anti-cancer and anti-inflammatory properties as secondary metabolites. Identified secondary metabolites contain lot of biological properties, we focused antimicrobial activities against human pathogens. (Fig. 1; Table 1).

The study highlights the novel approach of utilizing computational methods to screen and manage the drug discovery process using the plant extract. The results suggest that this approach could lead to the improvement of new and successful treatments for viral infections. Identified alkaloids are used for including pain relief, psychoactive effects, stimulation, anesthesia, and antibacterial agents. Additionally, glycosides also contain antibacterial properties. Tannins exhibit antibacterial properties that make them effective against bacterial infections, while phenolics possess strong antioxidant capacity that combats free radical production in the body. These plant metabolites offer promising health benefits [20]. The potential of these natural resources for therapeutic applications, *Black liquor* from traditional alkaline cellulose extraction contains phytochemicals with multiple applications [21].

### 4.2 Total Phenol Content (TPC)

In total phenolic content analysis of ethanolic leaf extract of *E. crassipes* plant used the well-known Folin–Ciocalteu technique. the highest TPC value was observed that 212.47 ± 7.07 mg $GAE^{-1}$. These exogenous cell reinforcements are regularly called "nourishing cancer prevention agents." Cell fortifications benefit the body by killing and expelling free radicals from the circulatory framework (Table 2).

### 4.3 Compounds identification by GC–MS of *E. crassipes*

In ethanolic leaf extract the 12 bioactive compounds are identified, retention time ranging in (RT) from 8.95 to 38.87. The highest RT compound was identified as 17-Pentatriacontene, while the lowest RT compound was Cyclohexasiloxane and dodecamethyl. Notably, Phytol, 9,12,15-Octadecatrienoic acid, and Hexadecanoic acid methyl ester remained identified compounds are pharmacological activity potential, similar compounds previously reported in other species of *E. crassipes* plant. The results of the GC–MS analysis were further analyzed using histogram analysis to obtain a more detailed understanding of the chemical profile of the *E. crassipes* sample (Fig. 2; Table 3).

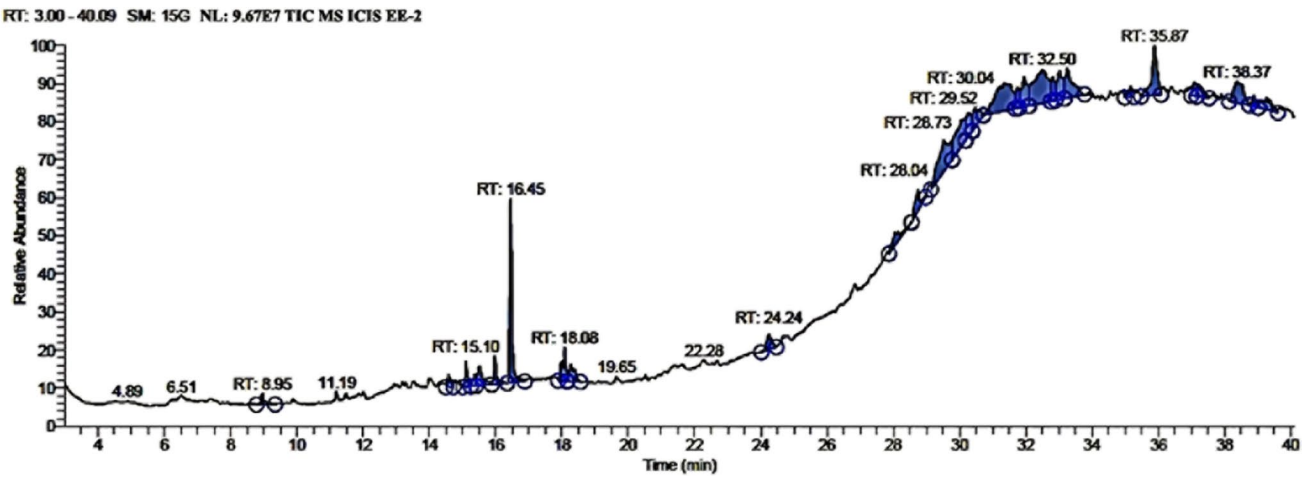


**Fig. 2** Histogram analysis of GC–MS of ethanolic leaf extract of *E. crassipes*

**Table 3** Analysis of GC–MS of *E. crassipes*

| | List of Compounds | Retention time | Molecular Formula | Molecular weight g/mol | Bio activity |
|---|---|---|---|---|---|
| 1 | Cyclohexasiloxane, dodecamethyl | 8.95 | $C_{12}H_{36}O_6Si_6$ | 444 | Anti-inflammatory and human pathogen [22] |
| 2 | Phytol | 15.10 | $C_{20}H_{40}O$ | 296 | Anti-bacterial [23] |
| 3 | Hexadecanoic acid, methyl ester | 15.97 | $C_{17}H_{34}O_2$ | 270 | Anti-cancer and inflammation [24] |
| 4 | Dibutyl phthalate | 16.45 | $C_{16}H_{22}O_4$ | 278 | Cyto-toxicity [25] |
| 5 | Tetracosamethyl-cyclododecasiloxane | 24.24 | $C_{24}H_{72}O_{12}Si_{12}$ | 889 | Anti-fungal assay [26] |
| 6 | Hexasiloxane | 29.52 | $O_5Si_6$ | 248 | Anti-bacterial and cyto-toxic [27] |
| 7 | 9,12,15 Octadecatrienoic Acid | 30.24 | $C_{18}H_{30}O_2$ | 278 | Anti-microbial assay [28] |
| 8 | Octasiloxane | 32.81 | $C_{32}H_{72}O_{12}Si_8$ | 873 | Anti-oxidant [29] |
| 9 | Stigmasterol | 35.87 | $C_{29}H_{48}O$ | 412 | Hypo-cholesterol emic [30] |
| 10 | Acetic acid | 37.19 | $C_2H_4O_2$ | 60 | Chemopreventive and pesticides [29] |
| 11 | Oleic acid, eicosyl ester | 38.37 | $C_{38}H_{74}O_2$ | 563 | Anticancer [31] |
| 12 | 17-Pentatriacontene | 38.37 | $C_{35}H_{70}$ | 490 | Antimicrobial [32] |

The investigation of the bioaccumulation capacities of *E. crassipes* focused on four different types of compounds:pentabromodiphenyl ether (1), di-n-hexyl phthalate (2), acetamiprid (3), nitenpyram and (4). Compound 1 is a monomer utilized in plastic production, while compound 2 is a flame retardant. Both compounds is known to been docrine-disrupting substances. On the other hand, compounds 3 and 4 are neonicotinoid insecticides that are neurotoxic. All four compounds have aromatic cycles and share similarities with phthalates. *E. crassipes* was found to have the capacity to accumulate these pollutants [33, 34]. GC–MS analysis of mentha leaf extract methanol solvents are namely (±) neoisomethanol (±) [R.T-24.3] is methanol is two enantiomer couples of peppermint and (1R,3S,4S)-(+) neo methanol seven mins plant sample (1R,3R,4S)-(-) methanol showing on the biological activity of antimicrobial properties [35]. Showing on *Murraya koenigii* plant on [R.T 23.5] 4,5-dihydro (3.68%) the bioactive compounds and majority of mixer *C.gigantea* plants using secondary [R.T 23.5] 1-Hexadecyne (51.92), cyclohexane (3.45) and L-Glutamic acid (49.87), the biological activity of anti-cancer and anti-diabetic[32]. Showing on *Achillea millefolium* flower extract in GC–MS analysis identify of namely 7 monoterpene ketone 35.74% and alcohols 41.02%, Sesquiterpene hydrocarbons 2.62% and ketones 0.39%, 5.32% biological activity of alcohols and essential oil analysis of phytocompounds. The *S.marianum* plant ethanol extract contains bio-active compounds [R.T-19.7], namely α-pinene 24.5% and γ-cadinene 49.8% analysis of fatty acids composition is the predominance of oleic 30.2% and linoleic 50.5% acids are major compounds of hydrocarbon, steroids, fatty acids and presence of plant extract *P.farcta* genetic resources of purification and development natural anti-oxidant in biomedicine food chemicals which on 99.4%, 99.2% and 99.1% biological property of antioxidant activity [36]. Upon analyzing the methanolic root extract of *E.crassipes* using GC–MS, analysis of Di-n-hexyl phthalate 1 was detected at a retention time of 4.88 min.Additionally, an observed characteristic fragment in the phthalate structure (ion C8H4O34) at 148.84 indicated its presence. Furthermore, a co-injection of the extract with the marketable bioactive compound di-n-hexyl phthalate was conducted, resulting in yielding supported this interpretation, as reported [34]. Four phenolic compounds were identified in the extract of Sharlyn melon peels, namely, coumaric acid, vanillin, chlorogenic acid, and 4-hydroxybenzoic acid. Gas chromatography-mass spectrometry (GC–MS) analysis was conducted to identify the chemical composition of the samples. The GC–MS results revealed the presence of various compounds with potential biological activity, including isovanillic acid, luteolin-7-O-glucoside, quercetin-3-galactoside, neochlorogenic acid, chlorogenic acid, apigenin-7-glucoside, and 3-hydroxybenzoic acid. These compounds have been reported to possess antioxidant, anti-inflammatory, and antimicrobial properties, indicating their potential for beneficial biological effects [37]. The presence of in the extract confirms the ability of *E. crassipes* to bioaccumulate this compound, in line with our initial hypothesis.

### 4.4 UV–Visible Spectrophotometer

The bioreduction of AgNPs was evaluated using the UV visible technique. The AgNPs synthesis confirmation based on the observation of an absorption band at 448 nm, which corresponds to the surface plasmon resonance (SPR) phenomenon exhibited by the Ec-AgNPs. The development of

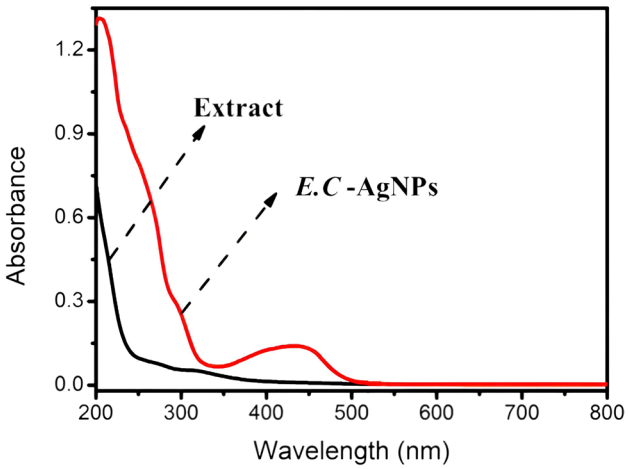


**Fig. 3** Analysis of *E.* c-AgNPs UV – wavelength

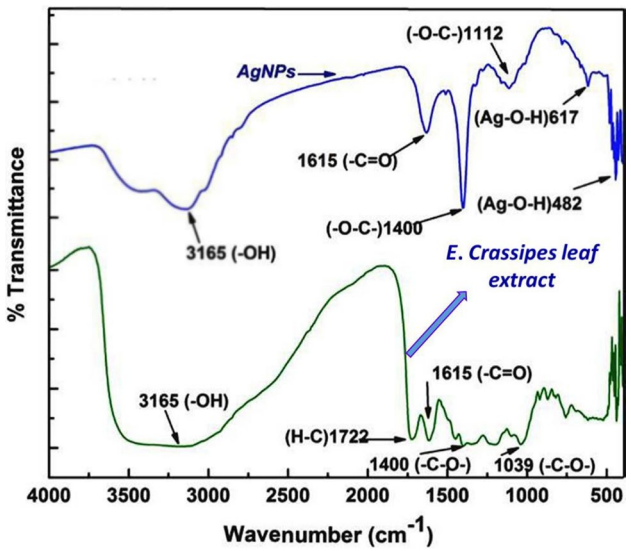


**Fig. 4** FT-IR analysis of synthesized *Es*-AgNPs

observation indicates the successfully synthesized of AgNPs formation (Fig. 3).

The plant extraction carried out the *Rumex dentatus Ru*-AgNPs green synthesized was confirmed by the observed color change and UV visible which (PDI) value of 0.754 in Poly-Dispersity Index) as a size distribution of AgNPs was analyzed using dynamic light scattering (DLS).These findings are consistent with a recent study conducted [38]. The UV–Vis absorption spectrum of synthesized AgNPs exhibited a prominent peak at 454 nm, atom-to-metal transition indicating the presence of surface plasmon resonance. This finding is consistent with previous reports on nanoparticles of different sizes, as documented [39]. In another study, *flax* seed extract was used for the successful synthesis of AgNPs, synthesized was confirmed by the observation of surface plasmon resonance A single broad peak at 530 nm emerged after 25 min of synthesizing the AgNPs, as documented in the study. This peak indicates the presence of the silver nanoparticles and confirms their successful formation [40].

### 4.5 FT-IR analysis of Ec-AgNPs synthesized

FTIR spectrometry was performed of *E. crassipes* leaf extract and synthesized AgNPs, in FTIR spectra the sample displayed characterization of peaks, indicating the occurrence of polyphenolic compounds. Strong evidence for the presence of these compounds was observed through the peaks at 3165 $cm^{-1}$ (–OH stretching), 1722 $cm^{-1}$ (–C–H stretching), 1615 $cm^{-1}$ (–C = O stretching of –COOH group of polyphenols), 1039 $cm^{-1}$ and 1400 $cm^{-1}$ (–C–O stretching). These identified polyphenolic compounds are likely to composition a vital character in the bioreduction process of silver nitrate, facilitating the formation of AgNPs. In a similar manner, the FTIR spectra of the AgNPs displayed peaks at 3165, 1615, and 1400 $cm^{-1}$, which corresponded to the stretching of –OH, –C = O, and –O–C–, respectively. These findings served as additional confirmation of the presence of polyphenolic compounds on the surfaces of the AgNPs. Furthermore, the presence of a peak at 1112 $cm^{-1}$ indicated the stretching of –C–O bonds, while the peaks at 617 $cm^{-1}$ and 482 $cm^{-1}$ suggested the existence of an –O–H bond between the oxygen atom of $Ag_2O$ and the hydrogen particle of the phenolic compound on the nanoparticle surface. These additional observations provided further support and confirmation regarding the presence of AgNPs (Fig. 4).

Analysis of FT-IR was conducted on *Es*-AgNPs to identification functional group, is a accountable for capping and reduction of nanoparticles. The result absorption bands was spectra exhibited at 3455, 1672, 1428, 1109, 850, and 619 $cm^{-1}$ [41]. The FTIR analysis of the biosynthesized *Es*-AgNPs revealed the occurrence of phytocompounds that could Performance such as caping agents, as indicated by the primary absorption bands observed at 3392, 1527, 1361, 1032, 832, and 647 $cm^{-1}$[42]. Notably, a shift in the band absorption at 3455 $cm^{-1}$ to 3392 $cm^{-1}$ was detected, which can be attributed absorption bands present in the phenolic compounds can be attributed to the NH bondthis suggests the participation of these compounds in the form of reduction and maintenance of the synthesized *Es*-AgNPs [43, 44]. The FTIR analysis of *Ca*-AgNPs showed shifts in various absorption bands compared to the leaf extract. Specifically, the band observed at 2995 $cm^{-1}$ was attributed to the stretching C-H vibration of the methylene group or aliphatic and triterpenoid, saponins, was observed. The band observed

at 1672 $cm^{-1}$, which indicates the stretching vibration of aromatic C = C bonds, shifted to 1527 $cm^{-1}$. Additionally, the peak observed at 1428 $cm^{-1}$ shifted to 1361 $cm^{-1}$, indicating the occurrence of tertiary alcohols with C-O stretching. Furthermore, the absorption peak observed at 1109 $cm^{-1}$ shifted to 1032 $cm^{-1}$, indicating the occurrence of stretching O–H vibration in the phenolic compounds. These shifts in the absorption bands signify changes in the functional groups and molecular environment during the *Ca*-AgNPs, synthesiszed of indicating the involvement of different chemical species and interactions in the realization and stabilization from the nanoparticles [45]. The functional groups O–H and N–H have a strong affinity for metal ions, making them essential in oxidation processes. Chitosan and polyphenolic compounds derived from algae FTIR spectroscopy is utilized to analyze functional groups in compounds, providing insights into their chemical composition and potential activities. Phlorotannins, such as dieckol, phloroglucinol, and eckol, exhibit characteristic FTIR bands indicating the presence of electron-donor amine groups (-NH2) and hydroxyl groups (-OH). These functional groups are associated with antioxidant, antimicrobial, and anti-inflammatory properties. Analyzing the FTIR bands of compounds like dieckol, phloroglucinol, and eckol offers valuable information about their potential activities based on their specific functional groups of the compounds contain a substantial amount of these groups, which contribute to their reactivity with metal ions [46, 47]. The secondary metabolites of plant extract *E. crassipes* leaf exposed the occurrence of polyphenols,tannins, alkaloids, steroids, and triterpenoids, which were utilized in the diminution of silver nitrate to AgNPs- *E. crassipes*.

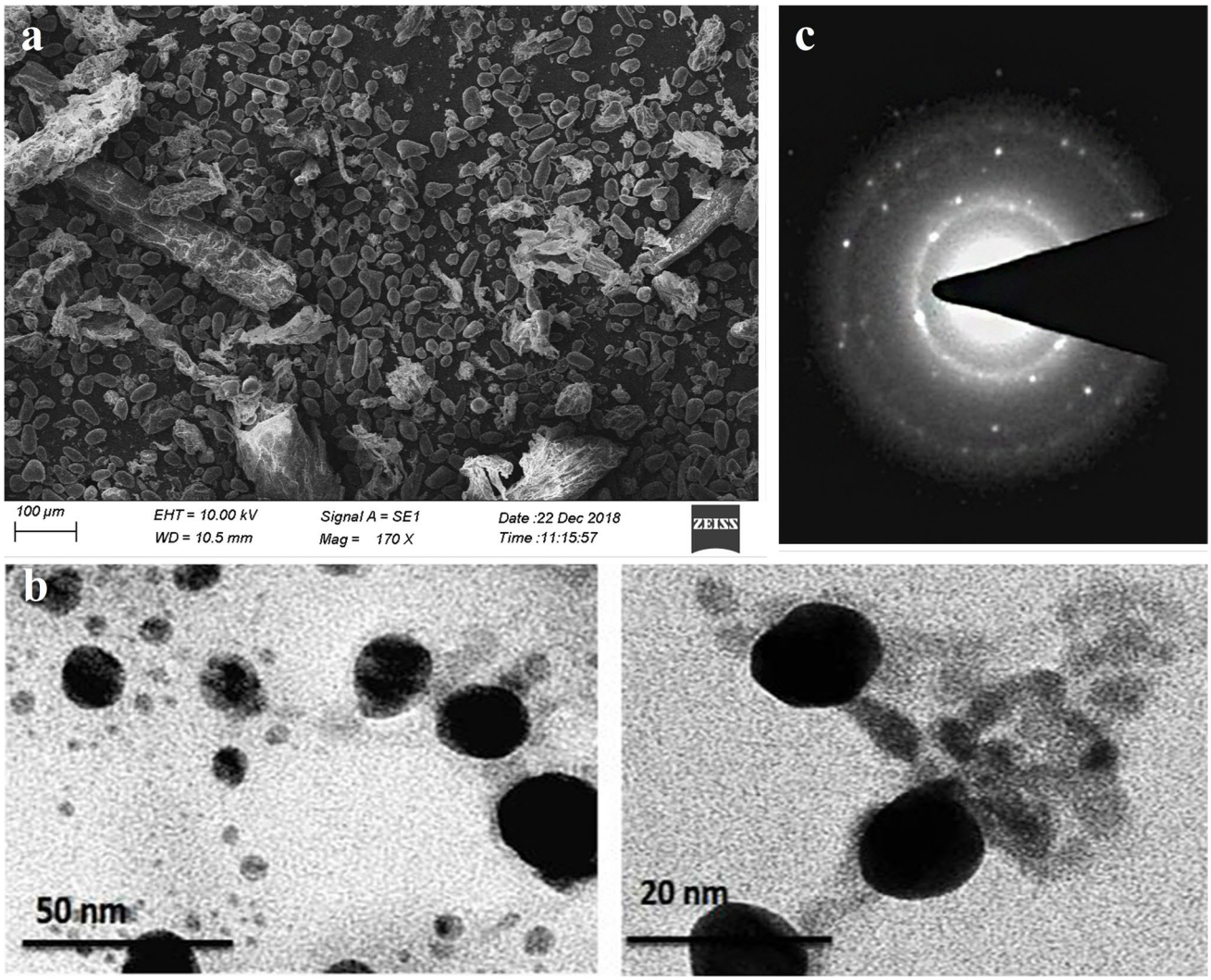


**Fig. 5** Synthesized AgNPs characterized by (**a**) SEM, (**b**) TEM, (**c**) SAED of *E.crassipes*

### 4.6 Structural characterization of SEM, TEM, SAED of *E. crassipes* leaf ethanolic extract

The structural study carried out on *E. crassipes* leaf ethanolic extract [FCC-Centered Cubic] of XRD pattern of biosynthesized, SEM of AgNPs analysis of particle size of 11 nm emission is examined on the surface of morphological and characterization analysis of AgNPs in the form of average in diameter 50–20 nm. In TEM, the analysed components in homogeneous polycrystalline potential shapes and showing on lattice spacing are 0.295 with spacing values (Fig. 5).

SEM images confirmed that the Ag NPs had an irregular morphology with size ranges of 20–80 nm, and a random spherical shape was observed [48]. The morphological characterization of using SEM structure, shape and sizesynthesized of silver nanoparticles (AgNPs) were analyzed [49]. The characterization of 25 nm size and a spherical shape were formed usingplant extraction *Boerhaaviadiffusa* of silver nanoparticles (AgNPs) synthesized [50]. Showing on TEM images revealed synthesized of nanoparticles (Nps) were spherical, polydispersed, and well-crystallized [51]. It is a commonly used technique in medicinal applications. The analysis of AgNPs synthesized from *E. crassipes* leaves revealed an estimation of their potential as a good source for glycol-oxidative damage protection. The synthesized silver nanoparticles using kraft lignin from the hardwood fraction as a stabilizing agent without the utilize of chemical reagents. The synthesized of (AgNPs) silver nanoparticles using were particle size at 24.7 nm and showed antimicrobial activity under microwave irradiation [52]. Phenolic compounds with higher levels of hydroxylation in their chemical structures exhibit enhanced capacity for scavenging radicals and a greater tendency to reduce Ag + to AgNPs. Additionally, when chitosan and polyphenols are combined, they synergistically enhance the bactericidal properties of biogenic AgNPs [9, 53]. Synthesized AgNPs confirmed on cellulose Nanocomposite, particle size ~ 24 nm in spherical shapes [54]. Green synthesized silver nanoparticles (AgNPs) remain spherical cutting-edge shape with an average diameter size of 32.75 nm were obtained using *Naringi crenulata* leaf ethanol extract. The morphological characterization showed the spherical shape. The AgNPs exhibited significant (AgNPs) Green-synthesized nanoparticles exhibit potent anti-bacterial activity against multidrug-resistant bacteria [55]. Copper oxide were synthesized of nanoparticles utilizing *E. crassipes* (Water hyacinth) leaf extract an environmentally friendly approach of a size range of 10–100 nm they are resulting nanoparticles exhibited [51].

### 4.7 XRD, EDX and AFM characterization of synthesized AgNPs of *E.crassipes*

Based on XRD patterns the synthesized silver nanoparticles (AgNPs) had crystalline structures, with narrow diffraction peaks at four Bragg reflections. In EDX designated that the irregular shapes of Ag-NPs were formed by the major elements of silver (70.2%), copper (28.80%), and oxygen (0.89%),

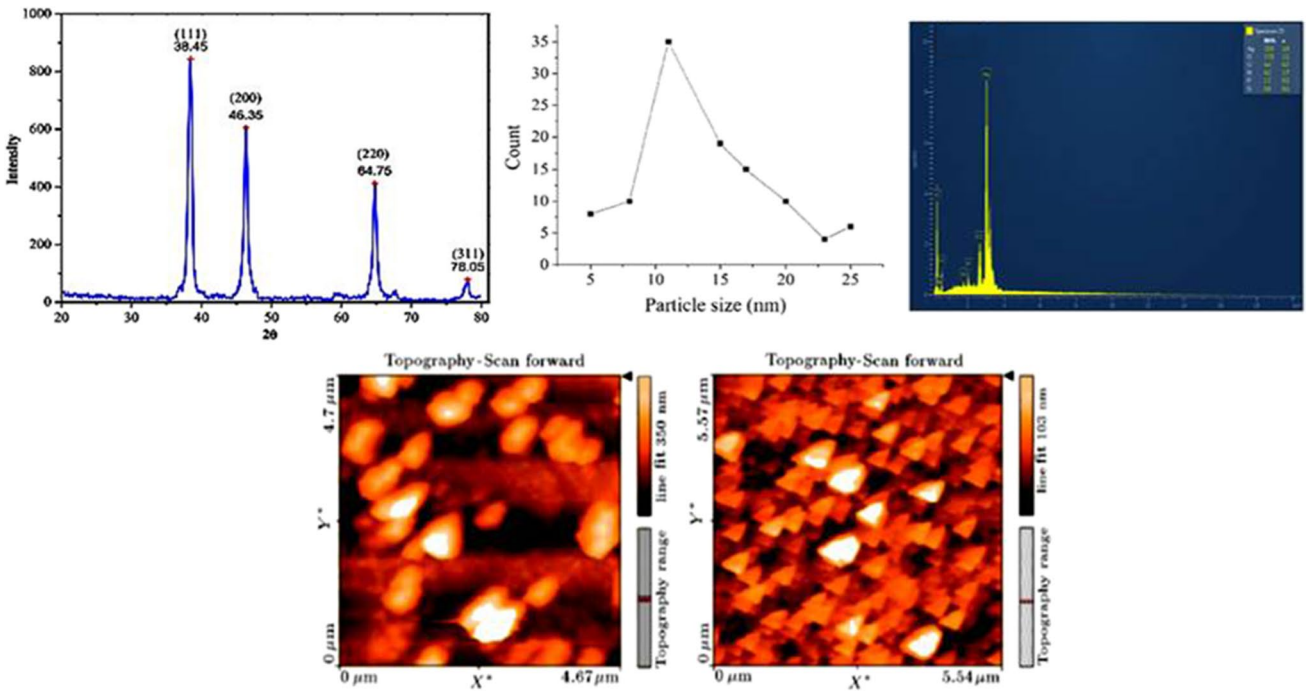


**Fig. 6** Synthesized AgNPs characterization by (**a**) XRD, (**b**) EDX and (**c**) AFM

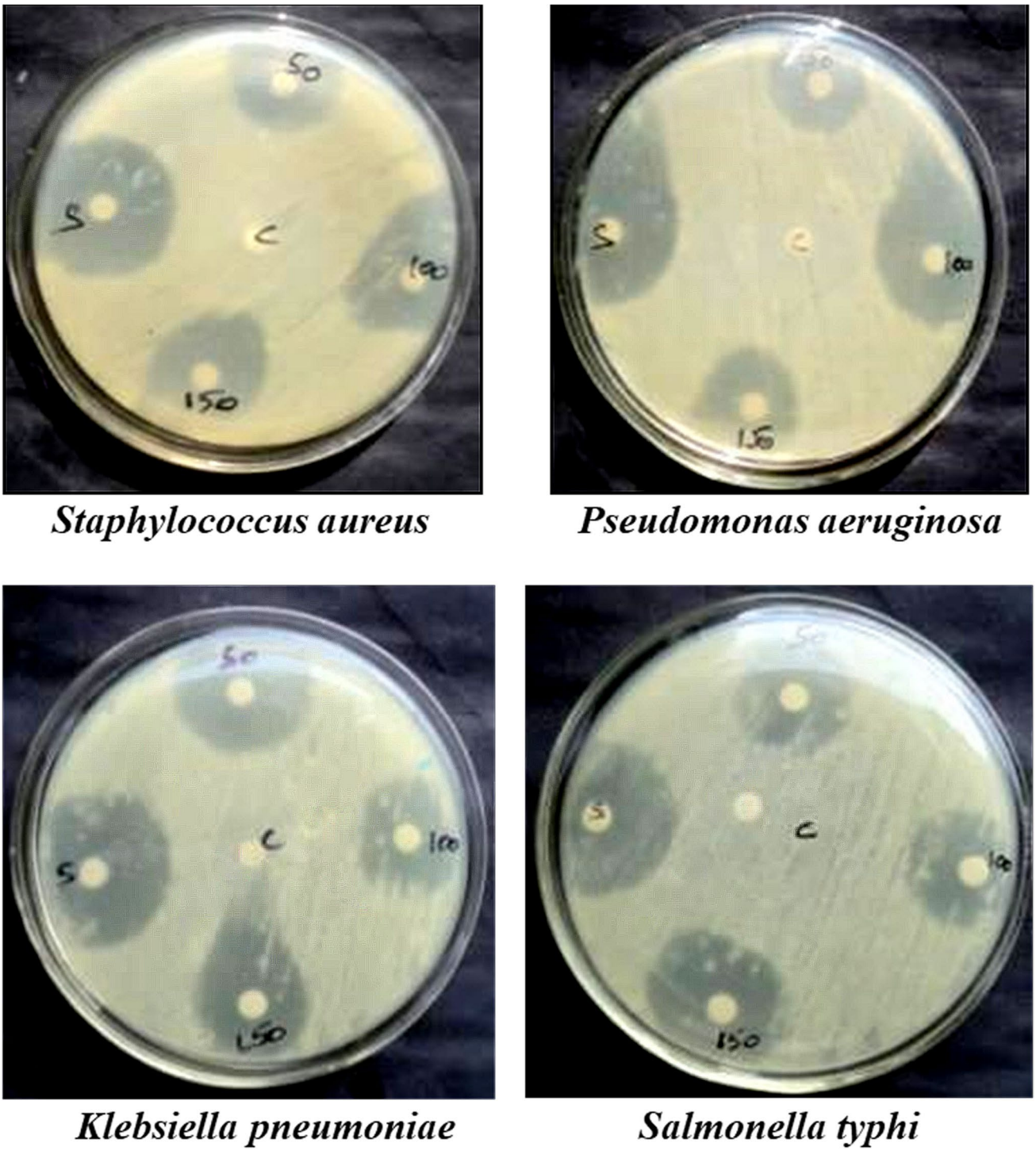


**Fig. 7** Antibacterialpotential of the synthesized AgNPs

along with other biomolecules on the surfaces of silver. AFM images showed irregular shapes and sizes of synthesized silver nanoparticles utilized at 36–46.5 nm stretched, with an average size at 46.5 nm. These findings indicate that *E. crassipes* serve as a valuable source for silver nanoparticle synthesizing with potential applications in various fields (Fig. 6).

XRD analysis of *Persea americana* seed aqueous extract revealed diffraction peaks at (210), (111), (200), (220), (311), and (222), indicating AgNPs synthesized crystal structure was analyzed [56]. Aqueous leaf extract of *Anacardium occidentale* plant was utilized the synthesis of bimetallic nanoparticles (BMNPs) with a ratio of Au/Ag: 1:1. XRD analysis of the

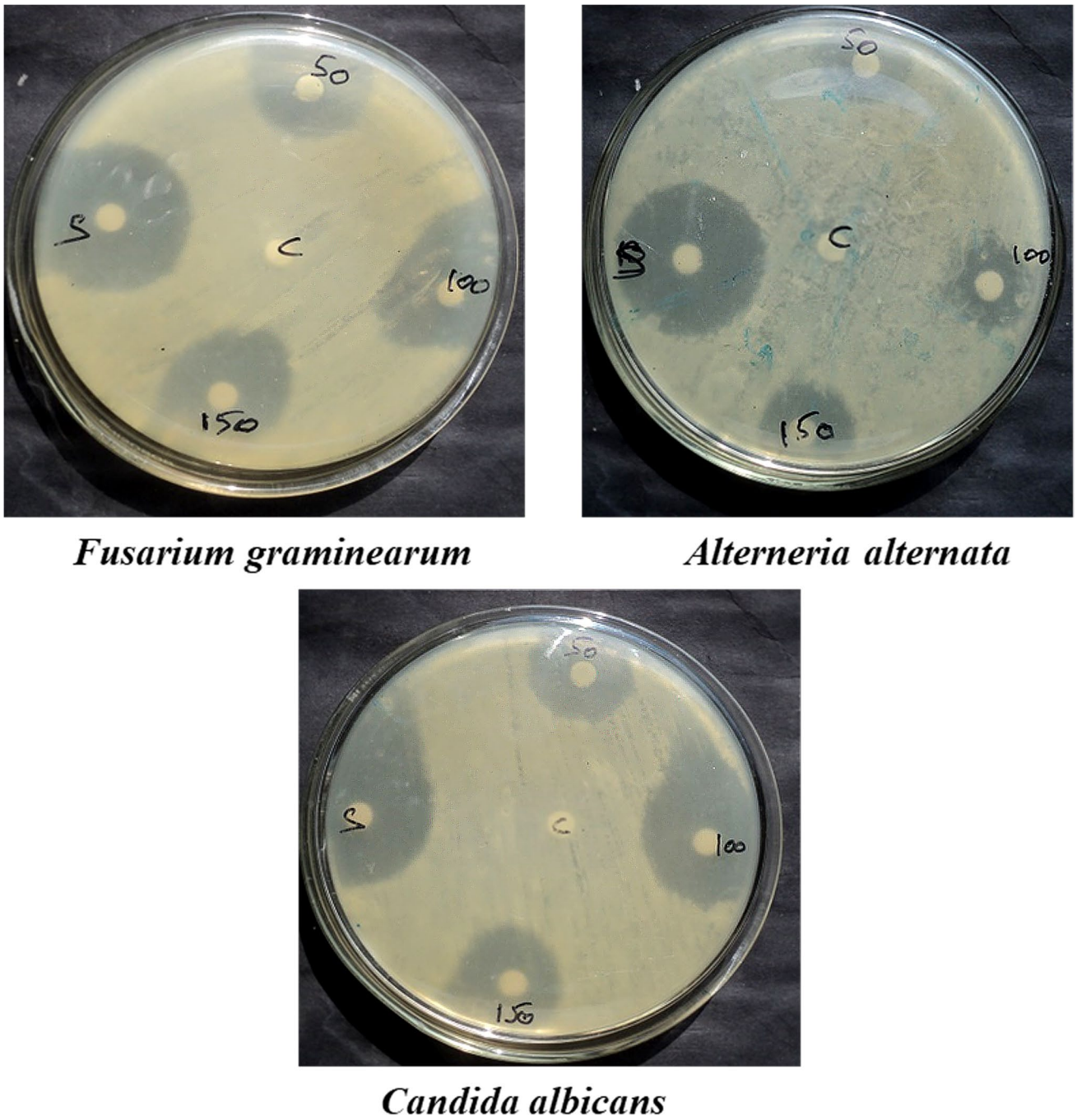


**Fig. 8** Antifungalactivity of synthesized AgNPs

BMNPs revealed prominent peak values at (111), (200), (220), and (311), confirming their crystalline nature [57]. *Tagetes erecta* extracts analysis revealed the synthesis of FCC silver nanoparticles (AgNPs) with a crystallite size of 11.87 nm, its confirmed by XRD pattern analysis [58]. The synthesis of Zinc oxide nanoparticles involved characterization of their structure and chemical properties using Miller indices and crystallographic planes. XRD analysis revealed a pattern position of peaks without significant differences in peak intensity, with high peaks value at 2θ values of 38.49°, 44.09°, and 78.31° for reflections, indicating potential applications in thermo-fluids industries. The antibiotic cefotaxime was also tested for its effect on the nanoparticles, and both showed peaks at the same values as the standard card [59]. Characterization of *Terminalia arjuna* and *Thespesia populnea* fruits extracts revealed high purity of elemental constituents and dominant peaks, AgNPs

synthesized were employed catalyst photo-degradation of B dye, specifically Rhodamine[60].

XRD analysis was performed to the presence of both amorphous and crystalline matrices before and after adsorption. Prior to adsorption, distinct high-intensity peaks were observed at 2θ angles of 15°, 23°, 28°, 41°, 50°, and 67°. After adsorption, a significant number of peaks were detected at 2θ angles of 15°, 24°, 29°, 36°, 40°, 43°, 47°, 64°, and 77°. The presence of these intense peaks in both analyses indicates the presence of a crystalline structure, as confirmed by the obtained results. [61]. Finally, AFM analysis was conducted, which showed the spherical shape of biosynthesized AgNPs layered with a thin film on thick aluminum foil using material the *E. crassipes* plant. The analysis also revealed the presence of both impure and highly pure nanoparticles.

### 4.8 Antibacterial activity Potential of Synthesized Ag NPs

AgNPs demonstrated effective antibacterial activity against four strains of human pathogenic bacteria such as *Salmonella typhi, Pseudomonas aeruginose, Staphylococcus aureus,* and *Klebsiella Pneumonia*. The synthesized silver nanoparticles (Ag NPs) demonstrated potent antimicrobial activity against *Staphylococcus aureus*; as evidenced by a zone of inhibition measuring from the $16.8 \pm 0.03$ mm at a high concentration 80 µg/mL (Fig. 7). The antimicrobial properties of AgNPs need remained extensively studied, with amoxicillin commonly used as a standard [62]. However, in one study, none of the synthesized Ag NPs showed a higher inhibition zone than the standard antibiotic, although the maximum zone of inhibition was observed by increasing the concentration of Ag NPs [63, 64]. This study evaluated the antimicrobial activity of Ag NPs against *E. coli; P. aeruginosa; S. aureus;* and *B. subtilis* at different concentrations of ranging from 5 µg/mL to 40 µg/mL. The results showed that *S. aureus* exhibited strong antimicrobial resistance to AgNPs at different concentrations [18, 65].

This study aimed to assess the efficacy of a specific intervention or treatment involving (AgNPs) silver nanoparticles synthesized from *Hibiscus* flowers against *Staphylococcus aureus; Escherichia col;, Vibrio cholera*; and *Klebsiella pneumonia* [66]. The synthesized silver nanoparticles (AgNPs) demonstrated remarkable antibacterial activity, exhibiting the greatest zone of inhibition at a concentration of 100 µg/mL. These findings highlight the potent effectiveness of the AgNPs in suppressing bacterial growth. Furthermore, the antibacterial activity against the different pathogens exhibited a dose-dependent response.

### 4.9 Antifungal Activity of Synthesized Ag NPs

The antifungal properties of synthesized AgNPs against multiple fungal pathogens are *Candida albicans; Alternaria alternata;* and *Fusarium graminium*. The antifungal efficacy of synthesis AgNPs was evaluated using the agar dilution technique, with fluconazole serving as a standard drug for comparison. The findings of the study indicated demonstrated of effectiveness on the AgNPs against all three fungal strains. *Fusarium graminium* exhibited the highest the inhibition observed zone of $12.1 \pm 0.01$ mm at a concentration of 80 µg/mL. Minimum inhibition zones of $9.8 \pm 0.04$ mm and $10.7 \pm 0.03$ mm were observed against *Alternaria alternata* and *Candida albicans*, respectively, also at a concentration of 80 µg/mL. These findings highlight indicate the synthesized AgNPs particals hold potential as findings demonstrate the effectiveness antifungal agents against a diverse range of fungal strains (Fig. 8). The mechanism of action of silver-based nanoparticles involves binding of Ag + ions to the thiol group of different proteins, which denatures them and leads to inhibition of DNA replication and microbial death. Furthermore, the nanoparticles induce alterations of cell layer and modify shapes of electron-thick granules through interaction with sulphur [67]. Research has shown that increasing the concentrations of AgNPs significantly inhibits the growth of fungi [68]. Additionally, several studies have shown significant antifungal activity of the synthesized AgNPs. To evaluate their antifungal potential, the AgNPs were tested against selected pathogenic fungi, including *F. oxysporum; C. albicans; C. glabrata; and A. alternata.* Among these, the lowest antifungal activity was observed against *C. albicans;* followed by *C. glabrata* and *F. oxysporum* [69]. These findings suggest that silver-based nanoparticles important implications for the development of new antimicrobial drugs in pharma industries.

Environment Ag NPs synthesis of human energy metabolites and Environmental factor and anti-microorganism using from green synthesis (AgNPs) synthesized.

## 5 Conclusions

The ethanolic leaf extract of *E. crassipes* focused different secondary metabolites by qualitative methods identified alkaloids, phenols, flavnoids etc., with this extract and silver nitrate solution nanoparticles prepared. The effectiveness of AgNPs was confirmed through different characterization by various analytical techniques; includs UV, FT-IR, XRD, SEM, TEM, EDX, and AFM. In UV analysis confirmed nanoparticles, functional groups are identified by FT-IR, in

SEM analysis AgNPs size (11 nm) confirmed and identified. TEM analysis average size (20–50 nm) and spherical shape noticed. Further confirmation of nanoparticles by XRD EDX and AFM analyses morphology, synthesized nanoparticles and images show irregular shapes and sizes ranged (36–46.5 nm). Synthezied AgNPs of *E. crassipes* focused for antimicrobial activity of selected human pathogenic bacteria and fungus, confirmed very stong antimicrobial activity against pathogens. From our work we confirmed that selected plant potentially used for human society in related to pharma, medical industries.

**Acknowledgements** The mentioned statement indicates that the work is supported by the Department of Community Medicine at Saveetha Institute of Medical And Technical Sciences (SIMATS) in Chennai, Tamil Nadu, India.

**Authors Contribution** Azhagu Madhavan Sivalingam:- Work Designed, Writing –Original Draft, Writing-Review & Editing, Grammar Checking, Visualization, Methodology, Formal analysis and Investigation. Arjun Pandian:- Editing, Formal analysis, Methodology, Visualization. Sumathy Rengarajan:- Formal analysis and methodology. Raju Ramasubbu:- Funding sources and formal analysis. All the authors give final approval of the version to be submitted.

**Funding** The authors express their gratitude to the Department of Biotechnology, New Delhi, India (Grant Number: BT/PR29159/FCB/125/9/2018) for their financial support.

**Data Availability** No data was used for the research described in the article.

## Declarations

**Ethical Approval** Not applicable.

**Consent for Publication** Not applicable.

**Competing Interests** The authors declare no competing interests.

## References

1. Kumari K, Bauddh K (2023) Chapter 18 - Phytoremediation of inorganic contaminants from the aquatic ecosystem using Eichhornia crassipes. In: Shukla SK, Kumar S, Madhav S, Mishra PK (eds) Metals in Water. Elsevier, pp 353–368. https://doi.org/10.1016/B978-0-323-95919-3.00001-X
2. Nguyen DTC, Van Tran T, Nguyen TTT, Nguyen DH, Alhassan M, Lee T (2022) New frontiers of invasive plants for biosynthesis of nanoparticles towards biomedical applications: A review. Science of The Total Environment:159278
3. Soto KM, López-Romero JM, Mendoza S, Peza-Ledesma C, Rivera-Muñoz EM, Velazquez-Castillo RR, Pineda-Piñón J, Méndez-Lozano N, Manzano-Ramírez A (2023) Rapid and facile synthesis of gold nanoparticles with two Mexican medicinal plants and a comparison with traditional chemical synthesis. Mater Chem Phys 295:127109. https://doi.org/10.1016/j.matchemphys.2022.127109
4. Murphy JW, Guentzel JL (2023) Total mercury and methylmercury concentrations in water hyacinth (Eichhornia crassipes) from a South Carolina coastal plain river. Aquatic Botany 184:103597. https://doi.org/10.1016/j.aquabot.2022.103597
5. Das RK, Pachapur VL, Lonappan L, Naghdi M, Pulicharla R, Maiti S, Cledon M, Dalila LMA, Sarma SJ, Brar SK (2017) Biological synthesis of metallic nanoparticles: plants, animals and microbial aspects. Nanotechnol Environ Eng 2(1):18. https://doi.org/10.1007/s41204-017-0029-4
6. Usui H, Shimizu Y, Sasaki T, Koshizaki N (2005) Photoluminescence of ZnO nanoparticles prepared by laser ablation in different surfactant solutions. J Phys Chem B 109(1):120–124. https://doi.org/10.1021/jp046747j
7. Yan J, Abdelgawad AM, El-Naggar ME, Rojas OJ (2016) Antibacterial activity of silver nanoparticles synthesized In-situ by solution spraying onto cellulose. Carbohyd Polym 147:500–508. https://doi.org/10.1016/j.carbpol.2016.03.029
8. Fozia F, Ahmad N, Buoharee ZA, Ahmad I, Aslam M, Wahab A, Ullah R, Ahmad S, Alotaibi A, Tariq A (2022) Characterization and Evaluation of Antimicrobial Potential of Trigonella incise (Linn) Mediated Biosynthesized Silver Nanoparticles. Molecules 27(14):4618
9. Rezazadeh NH, Buazar F, Matroodi S (2020) Synergistic effects of combinatorial chitosan and polyphenol biomolecules on enhanced antibacterial activity of biofunctionalized silver nanoparticles. Sci Rep 10(1):1–13
10. Galdopórpora JM, Ibar A, Tuttolomondo MV, Desimone MF (2021) Dual-effect core–shell polyphenol coated silver nanoparticles for tissue engineering. Nano-Struct Nano-Objects 26:100716. https://doi.org/10.1016/j.nanoso.2021.100716
11. Pandian A, Semwal D, Semwal R, Malaiyandi M, Sivaraj C, Vijayakumar S (2017) Total Phenolic Content, Volatile Constituents and Antioxidative Effect of Coriandrum sativum, Murraya koenigii and Mentha arvensis. Nat Prod J 7:65–74. https://doi.org/10.2174/2210315506666161121104251
12. Khane Y, Benouis K, Albukhaty S, Sulaiman GM, Abomughaid MM, Al Ali A, Aouf D, Fenniche F, Khane S, Chaibi W (2022) Green synthesis of silver nanoparticles using aqueous Citrus limon zest extract: Characterization and evaluation of their antioxidant and antimicrobial properties. Nanomaterials 12(12):2013
13. Naseem K, Zia Ur Rehman M, Ahmad A, Dubal D, AlGarni TS (2020) Plant extract induced biogenic preparation of silver nanoparticles and their potential as catalyst for degradation of toxic dyes. Coatings 10(12):1235
14. Asgary V, Shoari A, Baghbani-Arani F, Shandiz SAS, Khosravy MS, Janani A, Bigdeli R, Bashar R, Cohan RA (2016) Green synthesis and evaluation of silver nanoparticles as adjuvant in rabies veterinary vaccine. Int J Nanomed 11:3597
15. Shah M, Nawaz S, Jan H, Uddin N, Ali A, Anjum S, Giglioli-Guivarc'h N, Hano C, Abbasi BH (2020) Synthesis of bio-mediated silver nanoparticles from Silybum marianum and their biological and clinical activities. Mater Sci Eng C, Mater Biol Appl 112:110889. https://doi.org/10.1016/j.msec.2020.110889
16. Sumra AA, Zain M, Saleem T, Yasin G, Azhar MF, Zaman QU, Budhram-Mahadeo V, Ali HM (2023) Biogenic Synthesis, Characterization, and In Vitro Biological Evaluation of Silver Nanoparticles Using Cleome brachycarpa. Plants 12(7):1578
17. Nagarajan S, Arjun P, Raaman N, Shah A, Sobhia ME, Das TM (2012) Stereoselective synthesis of sugar-based β-lactam derivatives: docking studies and its biological evaluation. Tetrahedron 68(14):3037–3045. https://doi.org/10.1016/j.tet.2012.02.017
18. Periasamy S, Jegadeesan U, Sundaramoorthi K, Rajeswari T, Tokala VNB, Bhattacharya S, Muthusamy S, Sankoh M, Nellore MK (2022) Comparative Analysis of Synthesis and Characterization of Silver Nanoparticles Extracted Using Leaf, Flower, and Bark of Hibiscus rosasinensis and Examine Its Antimicrobicidal Activity. J Nanomater 2022:1–10

19. Ali SG, Ansari MA, Alzohairy MA, Alomary MN, Jalal M, AlYahya S, Asiri SMM, Khan HM (2020) Effect of biosynthesized ZnO nanoparticles on multi-drug resistant Pseudomonas aeruginosa. Antibiotics 9(5):260
20. Al-Humaid A, Mousa H, El-Mergawi R, Abdel-Salam A (2010) Chemical composition and antioxidant activity of dates and dates-camel-milk mixtures as a protective meal against lipid peroxidation in rats. Am J Food Technol 5(1):22–30
21. Méndez-Loranca E, Vidal-Ruiz AM, Martínez-González O, Huerta-Aguilar CA, Gutierrez-Uribe JA (2023) Beyond cellulose extraction: Recovery of phytochemicals and contaminants to revalorize agricultural waste. Biores Technol Rep 21:101339. https://doi.org/10.1016/j.biteb.2023.101339
22. Tunnisa F, Nur Faridah D, Afriyanti A, Rosalina D, Ana Syabana M, Darmawan N, Dewi Yuliana N (2022) Antioxidant and antidiabetic compounds identification in several Indonesian underutilized Zingiberaceae spices using SPME-GC/MS-based volatilomics and in silico methods. Food Chemistry: X 14:100285. https://doi.org/10.1016/j.fochx.2022.100285
23. Rashed MMA, Mahdi AA, Ghaleb ADS, Zhang FR, YongHua D, Qin W, WanHai Z (2020) Synergistic effects of amorphous OSA-modified starch, unsaturated lipid-carrier, and sonocavitation treatment in fabricating of Lavandula angustifolia essential oil nanoparticles. Int J Biol Macromol 151:702–712. https://doi.org/10.1016/j.ijbiomac.2020.02.224
24. Dubois LM, Perrault KA, Stefanuto P-H, Koschinski S, Edwards M, McGregor L, Focant J-F (2017) Thermal desorption comprehensive two-dimensional gas chromatography coupled to variable-energy electron ionization time-of-flight mass spectrometry for monitoring subtle changes in volatile organic compound profiles of human blood. J Chromatogr A 1501:117–127. https://doi.org/10.1016/j.chroma.2017.04.026
25. Delaney P, Sarvothaman VP, Colgan R, Nagarajan S, Deshmukh G, Rooney D, Robertson PKJ, Ranade VV (2022) Removal of single and dual ring thiophene's from dodecane using cavitation based processes. Ultrasonics Sonochemistry 89:106148. https://doi.org/10.1016/j.ultsonch.2022.106148
26. Xiao N, Xu H, Jiang X, Sun T, Luo Y, Shi W (2022) Evaluation of aroma characteristics in grass carp mince as affected by different washing processes using an E-nose, HS-SPME-GC-MS, HS-GC-IMS, and sensory analysis. Food Res Int 158:111584. https://doi.org/10.1016/j.foodres.2022.111584
27. Su H, Kuang X, Ren Y, Luo L (2022) Biostimulants promote biodegradation of n-hexadecane by Raoultella planticola: Generation of lipopeptide biosurfactants. J Environ Chem Eng 10(5):108382. https://doi.org/10.1016/j.jece.2022.108382
28. Chen X, Cao J, Geng A, Zhang X, Wang H, Chu Q, Yan Z, Zhang Y, Liu H, Zhang J (2023) Integration of GC-MS and LC-MS for metabolite characteristics of thigh meat between fast- and slow-growing broilers at marketable age. Food Chemistry 403:134362. https://doi.org/10.1016/j.foodchem.2022.134362
29. Xu L, Cheng H, Müller M, Sinclair AJ, Wang W, Guo X, Vetter W, Wang Y (2023) Targeted quantitation of furan fatty acids in edible oils by gas chromatography/triple quadrupole tandem mass spectrometry (GC-TQ/MS). Food Chemistry 404:134521. https://doi.org/10.1016/j.foodchem.2022.134521
30. Li Y, Cao Z, Yu Z, Zhu Y, Zhao K (2023) Effect of inoculating mixed starter cultures of Lactobacillus and Staphylococcus on bacterial communities and volatile flavor in fermented sausages. Food Sci Human Wellness 12(1):200–211. https://doi.org/10.1016/j.fshw.2022.07.010
31. Azhagu Madhavan S, Sa V, Ra S, Sb R (2021) Phytochemical Screening and GC–MS Analysis Of Bioactive Compounds Present In Ethanolic Leaf Extract Murraya koenigii. Bull Env Pharmacol Life Sci 10:158–164
32. Madhavan SA, Vinotha P, Uma V (2020) Phytochemical screening and comparative gc–ms analysis of bioactive compounds present in methanolic leaf and latex extract Calotropis gigantea (L). Asian Journal of Advances in Medical Science:1–13
33. Shanab SM, Shalaby EA, Lightfoot DA, El-Shemy HA (2010) Allelopathic effects of water hyacinth [Eichhornia crassipes]. PLoS ONE 5(10):e13200
34. De Laet C, Matringe T, Petit E, Grison C (2019) Eichhornia crassipes: a Powerful Bio-indicator for Water Pollution by Emerging Pollutants. Sci Rep 9(1):7326. https://doi.org/10.1038/s41598-019-43769-4
35. Tian Y, Xu Z, Liu Z, Zhu R, Zhang F, Liu Z, Si X (2022) Botanical discrimination and classification of Mentha plants applying two-chiral column tandem GC-MS analysis of eight menthol enantiomers. Food Research International:112035. https://doi.org/10.1016/j.foodres.2022.112035
36. Taleghani A (2022) New bioactive compounds characterized by liquid chromatography-mass spectrometry and gas chromatography-mass spectrometry in hydro-methanol and petroleum ether extracts of Prosopis farcta (Banks & Sol) JF Macbr weed. J Mass Spectrometry: JMS 57(9):e4884–e4884
37. Ganji SM, Singh H, Friedman M (2019) Phenolic content and antioxidant activity of extracts of 12 melon (Cucumis melo) peel powders prepared from commercial melons. J Food Sci 84(7):1943–1948
38. Abdo MM, Abdel-Hamid MI, El-Sherbiny IM, El-Sherbeny G, Abdel-Aal EI (2023) Green synthesis of AgNPs, alginate microbeads and Chlorella minutissima laden alginate microbeads for tertiary treatment of municipal wastewater. Biores Technol Rep 21:101300. https://doi.org/10.1016/j.biteb.2022.101300
39. Henglein A (1993) Physicochemical properties of small metal particles in solution:" microelectrode" reactions, chemisorption, composite metal particles, and the atom-to-metal transition. J Phys Chem 97(21):5457–5471
40. Alzubaidi AK, Al-Kaabi WJ, Ali AA, Albukhaty S, Al-Karagoly H, Sulaiman GM, Asiri M, Khane Y (2023) Green Synthesis and Characterization of Silver Nanoparticles Using Flaxseed Extract and Evaluation of Their Antibacterial and Antioxidant Activities. Appl Sci 13(4):2182
41. Kumar D, Kumar G, Das R, Agrawal V (2018) Strong larvicidal potential of silver nanoparticles (AgNPs) synthesized using Holarrhena antidysenterica (L.) Wall. bark extract against malarial vector, Anopheles stephensi Liston. Process Safety and Environmental Protection 116. https://doi.org/10.1016/j.psep.2018.02.001
42. He Y, Wei F, Ma Z, Zhang H, Yang Q, Yao B, Huang Z, Li J, Zeng C, Zhang Q (2017) Green synthesis of silver nanoparticles using seed extract of Alpinia katsumadai, and their antioxidant, cytotoxicity, and antibacterial activities. RSC Adv 7:39842–39851. https://doi.org/10.1039/C7RA05286C
43. Qais F, Shafiq A, Khan H, Husain F, Khan RA, Alenazi B, Alsalme A, Ahmad I (2019) Antibacterial Effect of Silver Nanoparticles Synthesized Using Murraya koenigii (L.) against Multidrug-Resistant Pathogens. Bioinorg Chem Appl 2019:1–11. https://doi.org/10.1155/2019/4649506
44. Sabapathi N, Ramalingam S, Aruljothi KN, Lee J, Barathi S (2023) Characterization and Therapeutic Applications of Biosynthesized Silver Nanoparticles Using Cassia auriculate Flower Extract. Plants 12(4):707
45. Mickymaray S (2019) One-step Synthesis of Silver Nanoparticles Using Saudi Arabian Desert Seasonal Plant Sisymbrium irio and Antibacterial Activity Against Multidrug-Resistant Bacterial Strains. Biomolecules 9:662. https://doi.org/10.3390/biom9110662
46. Tomaszewska E, Soliwoda K, Kadziola K, Tkacz-Szczesna B, Celichowski G, Cichomski M, Szmaja W, Grobelny J (2013) Detection limits of DLS and UV-Vis spectroscopy in characterization of polydisperse nanoparticles colloids. J Nanomater 2013:60–60
47. Zhang D, Wang C, Shen L, Shin H-C, Lee KB, Ji B (2018) Comparative analysis of oxidative mechanisms of phloroglucinol and

dieckol by electrochemical, spectroscopic, cellular and computational methods. RSC Adv 8(4):1963–1972
48. Prabu HJ, Johnson I (2015) Plant-mediated biosynthesis and characterization of silver nanoparticles by leaf extracts of Tragia involucrata, Cymbopogon citronella, Solanum verbascifolium and Tylophora ovata. Karbala Int J Modern Sci 1(4):237–246
49. Chakravarty P, Sarma NS, Sarma H (2010) Removal of lead (II) from aqueous solution using heartwood of Areca catechu powder. Desalination 256(1–3):16–21
50. Sun Q, Cai X, Li J, Zheng M, Chen Z, Yu C-P (2014) Green synthesis of silver nanoparticles using tea leaf extract and evaluation of their stability and antibacterial activity. Colloids Surf, A 444:226–231
51. Saligedo TS, Muleta GG, Tsega TW, Tadele KT (2023) Green Synthesis of Copper Oxide Nanoparticles Using Eichhornia Crassipes Leaf Extract, its Antibacterial and Photocatalytic Activities. Curr Nanomater 8(1):58–68
52. Deeksha B, Sadanand V, Hariram N, Rajulu AV (2021) Preparation and Properties of Cellulose Nanocomposite Fabrics with in situ Generated Silver Nanoparticles by Bioreduction Method. J Biores Bioprod 6(1):75. https://doi.org/10.1016/j.jobab.2021.01.003
53. Bhutto AA, Kalay Ş, Sherazi STH, Culha M (2018) Quantitative structure–activity relationship between antioxidant capacity of phenolic compounds and the plasmonic properties of silver nanoparticles. Talanta 189:174–181. https://doi.org/10.1016/j.talanta.2018.06.080
54. Clichici S, David L, Moldovan B, Baldea I, Olteanu D, Filip M, Nagy A, Luca V, Crivii C, Mircea P, Katona G, Filip GA (2020) Hepatoprotective effects of silymarin coated gold nanoparticles in experimental cholestasis. Mater Sci Eng: C 115:111117. https://doi.org/10.1016/j.msec.2020.111117
55. Chinnathambi A, Alharbi SA, Joshi DVS, Jhanani GK, On-uma R, Jutamas K, Anupong W (2023) Synthesis of AgNPs from leaf extract of Naringi crenulata and evaluation of its antibacterial activity against multidrug resistant bacteria. Environ Res 216:114455. https://doi.org/10.1016/j.envres.2022.114455
56. Rajkumar G, Sundar R (2022) Biogenic one-step synthesis of silver nanoparticles (AgNPs) using an aqueous extract of Persea americana seed: Characterization, phytochemical screening, antibacterial, antifungal and antioxidant activities. Inorganic Chem Commu 143:109817. https://doi.org/10.1016/j.inoche.2022.109817
57. Sheny DS, Mathew J, Philip D (2011) Phytosynthesis of Au, Ag and Au–Ag bimetallic nanoparticles using aqueous extract and dried leaf of Anacardium occidentale. Spectrochim Acta Part A Mol Biomol Spectrosc 79(1):254–262. https://doi.org/10.1016/j.saa.2011.02.051
58. Katta VKM, Dubey RS (2021) Green synthesis of silver nanoparticles using Tagetes erecta plant and investigation of their structural, optical, chemical and morphological properties. Mater Today: Proceed 45:794–798. https://doi.org/10.1016/j.matpr.2020.02.809
59. Kumar R, Arora N, Gupta M, Katyal P (2022) An experimental approach on characterization techniques of zinc oxide nanoparticles. Mater Today: Proceed 56:2469–2477. https://doi.org/10.1016/j.matpr.2021.08.239
60. Amutha K, Grace Annapoorani S, Sudhapriya N (2020) Dyeing of textiles with natural dyes extracted from Terminalia arjuna and Thespesia populnea fruits. Industrial Crops Prod 148:112303. https://doi.org/10.1016/j.indcrop.2020.112303
61. Xue H, Wang X, Xu Q, Dhaouadi F, Sellaoui L, Seliem MK, Lamine AB, Belmabrouk H, Bajahzar A, Bonilla-Petriciolet A (2022) Adsorption of methylene blue from aqueous solution on activated carbons and composite prepared from an agricultural waste biomass: A comparative study by experimental and advanced modeling analysis. Chem Eng J 430:132801
62. Ovais M, Khalil AT, Raza A, Khan MA, Ahmad I, Islam NU, Saravanan M, Ubaid MF, Ali M, Shinwari ZK (2016) Green synthesis of silver nanoparticles via plant extracts: beginning a new era in cancer theranostics. Nanomedicine 12(23):3157–3177
63. Raut RW, Mendhulkar VD, Kashid SB (2014) Photosensitized synthesis of silver nanoparticles using Withania somnifera leaf powder and silver nitrate. J Photochem Photobiol, B 132:45–55
64. Feng QL, Wu J, Chen GQ, Cui F, Kim T, Kim J (2000) A mechanistic study of the antibacterial effect of silver ions on Escherichia coli and Staphylococcus aureus. J Biomed Mater Res 52(4):662–668
65. Periasamy S, Jegadeesan U, Sundaramoorthi K, Rajeswari T, Tokala VNB, Bhattacharya S, Muthusamy S, Sankoh M, Nellore MK (2022) Comparative Analysis of Synthesis and Characterization of Silver Nanoparticles Extracted Using Leaf, Flower, and Bark of Hibiscus rosasinensis and Examine Its Antimicrobicidal Activity. J Nanomater 2022:8123854. https://doi.org/10.1155/2022/8123854
66. Nayak D, Ashe S, Rauta PR, Nayak B (2015) Biosynthesis, characterisation and antimicrobial activity of silver nanoparticles using Hibiscus rosa-sinensis petals extracts. IET Nanobiotechnol 9(5):288–293. https://doi.org/10.1049/iet-nbt.2014.0047
67. Sridhara V, Pratima K, Krishnamurthy G, Sreekanth B (2013) Vegetable assisted synthesis of silver nanoparticles and its antibacterial activity against two human pathogens.
68. Pallavi S, Rudayni HA, Bepari A, Niazi SK, Nayaka S (2022) Green synthesis of Silver nanoparticles using Streptomyces hirsutus strain SNPGA-8 and their characterization, antimicrobial activity, and anticancer activity against human lung carcinoma cell line A549. Saudi J Biol Sci 29(1):228–238
69. Singh A, Dar MY, Joshi B, Sharma B, Shrivastava S, Shukla S (2018) Phytofabrication of silver nanoparticles: novel drug to overcome hepatocellular ailments. Toxicol Rep 5:333–342

**Publisher's Note** Springer Nature remains neutral with regard to jurisdictional claims in published maps and institutional affiliations.

Springer Nature or its licensor (e.g. a society or other partner) holds exclusive rights to this article under a publishing agreement with the author(s) or other rightsholder(s); author self-archiving of the accepted manuscript version of this article is solely governed by the terms of such publishing agreement and applicable law.